Geospatial Vegetation Dynamics Estimate Based on Multitemporal Remote Sensing at the Passaúna Basin

Jorge Antonio Silva Centeno [1], Mario Ernesto Jijón-Palma[2], Andressa Proença Cavassim[3]

[1] Geomatics Department, Federal University of Parana, Brazil – centeno@ufpr.br
[2] Geomatics Department, Federal University of Parana, Brazil – mario.jijon@ufpr.br
[3] Geodesic Sciences Postgraduate Program, Federal University of Parana, UFPR – Curitiba, Brazil – andressa.cavassim@ufpr.br

Keywords: multitemporal analysis. Binary encoding, vegetation, NDVI.

Abstract

This paper presents the results of a study aimed at analyzing land cover evolution—particularly vegetation—using remote sensing time series. The focus is on monitoring vegetation changes in the Passaúna basin, an important water supply source for Curitiba, Brazil. Vegetation in this basin plays a crucial role in ensuring both the quantity and quality of water available to the population. The study employed an unsupervised classification approach based on the Normalized Difference Vegetation Index (NDVI), combined with a binary encoding technique. A hybrid method was used, integrating classification results from multiple dates. The core of the methodology involved deriving indicators of seasonal or annual pixel variation by analyzing several images from the same year and comparing these indicators across different years. This approach enhanced the detection of seasonal land cover variations, thereby improving the identification of land cover classes. Using multiple observations per year proved especially effective in distinguishing different vegetation types. The analysis aimed to detect significant land cover changes, with particular emphasis on vegetation loss and recovery. The binary encoding technique facilitated the mapping of land cover evolution, especially changes associated with the filling of the Passaúna reservoir and helped pinpoint their locations. A key advantage of this method is that it does not require training sample selection for data classification. Because NDVI is a normalized index, variation ranges were used to separate certain land cover classes at each time point. The integration of multiple dates within a year increased the potential for accurate discrimination by capturing seasonal dynamics. From a hydrological perspective, the land cover changes observed between 1988 and 2018 were substantial, although the system has since shown signs of stabilization. The creation of the reservoir led to the emergence of new agricultural areas around the water body, while denser vegetation increased in the upper basin. These changes significantly affect infiltration rates and potential surface runoff, highlighting the hydrological impact of land cover dynamics in the region.

1. INTRODUCTION

To estimate the production of pollutants that reach a water body, the use of satellite images has become the most viable option for the quantification of different land cover and its role as pollution sources or filters. Traditional studies estimate the production of pollutants by digital multispectral image classification and thus obtaining a map of land cover in the drainage basin. This option is a limited solution as it only considers an instant in time for mapping the Earth's surface. However, agricultural practices, as well as the natural seasonal variations of vegetation themselves, imprint major changes in the scenario that can provide information about land cover classes, like agriculture or deforestation. Agriculture of varying species can be distinguished by the phenological cycle using several images along the season. This encourages the use of several images to improve the classification.

In the last decades, advances in image processing and the availability of image series facilitated the analysis of several images from the same place. Studies aimed at analysing the temporal variation and the dynamics of the land cover increased with the availability of historic series, like the Landsat collection, the Sentinel 2 mission, or the MODIS mission. The last one is interesting because of its high temporal resolution but the spatial resolution limits its use to map details, like agricultural fields.

The processing of long image time series enables the monitoring, visualization, and analysis of historical variations at the pixel level. This approach allows for the detection of abrupt changes—such as deforestation—as well as natural fluctuations linked to phenological cycles. Some methods that utilize extended time series focus on constructing functions that model the temporal evolution of each pixel, as seen in the work of Kennedy et al. (2010), who identified changes based on pixel trajectory analysis. To effectively build a representative historical series and analyse these temporal trajectories, high temporal resolution is preferred. However, achieving this resolution can be challenging due to the frequent presence of cloud cover in remote sensing imagery, which limits the availability of clear observations.

This study aims to use a time series of satellite images to quantify land cover dynamics, considering both natural variations in certain land cover types and changes driven by human activities. The analysis also seeks to detect significant changes—such as deforestation or land recovery—over time.

This contribution has been peer-reviewed. The double-blind peer-review was conducted on the basis of the full paper.
https://doi.org/10.5194/isprs-annals-X-3-W4-2025-63-2026 | © Author(s) 2026. CC BY 4.0 License.

Given that multitemporal studies typically involve numerous images, one of the study's objectives is to condense the temporal series into a single composite image. For this purpose, relevant information from each date in the series is encoded and integrated into a unified representation that summarizes the entire time span.

The study proposes a method for land cover classification and change detection based on binary encoding of NDVI (Normalized Difference Vegetation Index) time series. The goal is to evaluate the effectiveness of binary encoding in representing land cover dynamics and detecting temporal changes. Specifically, the study outlines the following objectives:
a) To propose methodologies for the multitemporal analysis of remote sensing image series.
b) To evaluate the feasibility of summarizing temporal dynamics using binary encoding.
c) To assess the potential of binary encoding in characterizing the temporal behaviour of specific land cover types.
d) To contribute to the generation of input data for hydrological models, particularly regarding land cover information.

2. LITERATURE REVIEW

The availability of the Landsat collection has opened the opportunity to carry out multitemporal studies with long image series. Like Hansen and Loveland (2012) point out, the availability of remote sensing products tends to grow. However, this requires the development of new multitemporal change detection methods. Methods that simultaneously analyse the pixel values of several images have been proposed in the literature, such as those proposed by Haywood et al. (2016), Cai and Liu (2015), or Kennedy et al. (2010).

Although it is desired to apply the concept of time series to remote sensing image collections, this task is not straightforward. Clouds and sensor failures can cause loss of data about the Earth's surface, making it difficult to obtain full and consistent data series. Authors like Chen et al. (2004) proposed methods to reconstruct remote sensing time series, recovering missing data and filling blanks. In a review about time series analysis, Fu et al. (2024) describe experiences that use approaches like the Savitzky–Golay filter, asymmetric Gaussian function, tensor-based models, or other fitting option, they state that they are not fully effective for filling large gaps. Concerning Machine Learning algorithms, they also point out that the low data availability is still a problem that restrains modelling the temporal dependency with sparce data.

The availability of long image series allows analysing the historical variation of each pixel in the image. This enables the detection of sudden changes due to major events, like deforestation, or natural oscillations resulting from the phenological cycle. Several works in the literature address the analysis of time series, such as Yuan et al. (2019); Rokni et al. (2014); Hu et al. (2015); Sheng et al. (2016); Taravat et al. (2016); Ogilvie et al. (2018); or Yao et al. (2019).

A common practice, as described in Li et al. (2021), is to monitor vegetation dynamics using the Normalized Difference Vegetation Index NDVI. An example can be found in Bertucini Jr. and Centeno (2017), who used the NDVI values to describe the temporal dynamics of agricultural fields in Brazil. A similar approach was used to map water bodies variations by Jijón-Palma et al. (2020), this time using the normalized difference water index (NDWI). Such studies summarize the temporal variations applying the concept of binary encoding described by Jia and Richards (1993) originally proposed to summarize hyperspectral image information. A similar approach is used in the present study to describe yearly land cover variations in the basin.

3. METHODS

The following are the steps of the methodology, which consist of the pre-processing of the images, the calculation of indexes, the coding of multitemporal information, and the analysis of changes.

Radiometric adjustments are necessary to grant accurate temporal analysis. The computation of surface reflectance values from the digital numbers of the multispectral image minimizes atmospheric and seasonal variability (Leonardo et al., 2006). Image registration errors can also produce significant differences, pointing out changes even in places where they do not occur.

For the experiments, it was used level 1 (T1) LANDSAT images, available at the USGS Earth Explorer site. Level 1 data includes corrected data, described as Level 1 Precision and Terrain (L1TP), radiometrically corrected, and intercalibrated between the different Landsat instruments. The geometric record of T1 scenes has low RMSE (root mean squared error) for the multispectral bands (USGS, 2023). These images are suitable for time series analysis and the basis for the research.

Figure 1 summarizes the encoding process and the classification step. The hybrid analysis consists of into two stages. In the first step it was computed the Normalized Difference Vegetation Index (NDVI, proposed by Townshend and Justice, 1986) for each image, using the red and near infrared bands. The NDVI varies between -1 and 1. Each NDVI image was segmented into four ranges using multiple thresholds that were derived from the literature. So, it became possible to code each segmented image using two bits. This procedure was repeated for the four images of the same year, obtaining four 2-bits images. The binary codes of each pixel were the concatenated to produce an 8-bits representation.

In the second step, the coded image was analysed to detect the most frequent codes and produce a land-cover thematic map. Finally, it was possible to compare the coded images to detect and analyse the changes.

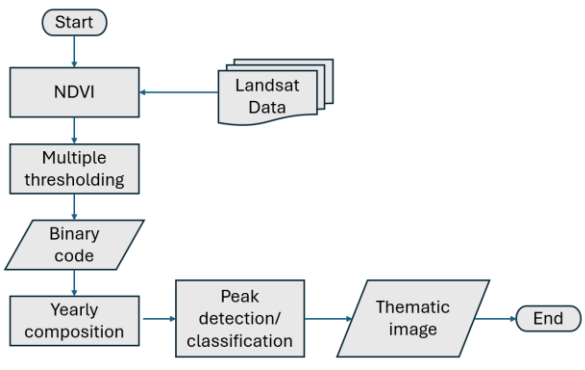

Figure 1 – Summary of the encoding and classification processes.

The proposed approach is a hybrid, procedure-based method that combines classification results from multiple dates. The aim is to leverage images from different times of the year to capture seasonal variations in land cover, which enhances the identification of cover types. The key advantage of using multiple observations per year lies in its ability to distinguish between vegetation types, detect variations in humidity, and identify the presence of water. However, a notable drawback is the increase in data volume, which leads to greater computational demands.

NDVI segmentation

To evaluate vegetation dynamics, the NVDI (Normalized Difference Vegetation Index), displayed on Equation 1, was computed from the red (RED) and near infrared (NIR) bands of the Landsat image (Townshend and Justice, 1986 and Tucker and Sellers, 1986). The NDVI, computed directly from satellite data, is related to vegetation canopy characteristics, such as biomass and percentage of vegetation cover. It is considered representative of the photosynthetic efficiency of plants and fluctuations due to changes in meteorological and environmental parameters (Gross, 2005).

$$NDVI = (NIR-RED) / (NIR+RED) \quad (1)$$

NDVI values vary between –1 and +1, and higher values represent a more vigorous and healthy vegetation, due to the high reflectance in the near infrared contrasting with the great absorption in the red region caused by the presence of chlorophyll in the leaf. The NDVI images were segmented using thresholds that were fixed based on previous research of Gross (2005) and Hashim et al. (2019).

Gross (2005) presents a multitemporal study to monitor the development of plant biomass in the Nile basin using time series of NDVI images. To separate different target classes based on the NDVI Gross (2005) proposes three ranges that can be identified in the NDVI:

- Very low values (0.1 or lower) are usually associated with rocks, sand and snow.
- Moderate values (0.2 to 0.3) found in shrubs and pastures.
- High values (0.6 to 0.8) associated with tropical and temperate forests.

The study of Gross (2005) was developed in a predominantly rural area. Elgammal et al. (2014) also used the NDVI to classify different types of coverage and for this purpose, they adjusted the thresholds to classify the index into three ranges. The most frequent values were areas without vegetation (below zero), little vegetation cover (0.0 – 0.3) and healthy vegetation (0.3-0.8). The authors recommend adapting these values for each case, although it is visible that the values are close to those proposed by Gross (2005).

Hashim et al. (2019) describe a similar study, for urban areas. These authors propose to segment the NDVI values according to the following intervals:

- Non-Vegetation: Areas of exposed soil, built-up area, road network (-1 - 0.199)
- Low Vegetation: Shrubs and pastures (0.2 - 0.5)
- High Vegetation: Temperate and tropical urban forest (0.501 - 1.0)

Comparing these two classifications (Gross, 2005 and Hashim et al., 2019), it is noted that gaps are present in the study by Gross (2005). This can be an advantage, as it restricts classification to regions with greater certainty, but on the other hand, it creates situations without classification. This is not the case with the schema of Hashim et al. (2019), which covers the entire spectrum of the index. Although the ranges are generally coincident in the two studies, the range between 0.4 and 0.6 deserves special attention. Here, Hashim et al. (2019) identify low (0.4-0.5) or high (0.5-0.6) vegetation. Gross (2005) does not specify any class, probably due to the possibility of mixing or this being a transition region.

Based on such experience, each image was segmented considering three range

- Non-vegetation: below 0.2,
- Low Vegetation 0.2 to 0.5 and
- High Vegetation, above 0.5.

The result is a thematic map with three classes (1, 2, 3), where the information of each pixel can be stored using two bits. Zero was left for water and other negative values.

Binary Code

Binary encoding is a practice used to summarize hyperspectral images, as described in Jia and Richards (1999) and has been adapted to summarize time series (Jijón-Palma et al., 2020). According to Xie et al. (2011), the use of binary encoding allows summarizing preserving the information to facilitate the interpretation of pixel dynamics.

Due to the high cloud cover in the region, only four dates were processed per year. The months with the lowest chance of clouds are March, April, July and October. For each month there are four possibilities (00, 01, 10 and 11), so 2 bits per date are necessary. When four dates are processed, eight bits are required. This means that the information of the NDVI of four images within a year, after classification, was stored in an 8-bits single image.

Temporal Dynamics Analysis

The result of binary encoding several images of one year is an image where the temporal dynamics are stored as an 8-bits digital number. To map the most frequent variations, the histogram of this image was computed. The histogram peaks revealed the most frequent digital numbers that can be found in the study area. The digital numbers of the largest peaks were then translated to vegetation temporal changes, as the binary code enables visualizing when vegetation is present in the pixel along the year. This enabled identifying land-cover classes that don't change along the year, like forests, or agriculture, characterized by low or no vegetation during some months and dense vegetation during other months. The analysis was repeated for several years, aiming at evaluating the land cover dynamics in the basin.

4. STUDY AREA

The Passaúna River is approximately 48 km long, with a drainage area of 217 km^2. It is a tributary of the Iguaçu River, covering the municipalities of Curitiba and Araucária, in Brazil, as displayed in Figure 2. This basin has low urban occupation, being predominantly rural (Cipriano et al., 2019). In this basin a reservoir was built for water supply. The Passaúna reservoir is in a heterogeneous and medium-sized basin (area of 8.4 km^2). This reservoir supplies water to the Metropolitan Region of Curitiba and, despite being a reservoir with a reasonable

environmental condition, episodes of cyanobacterial bloom were already observed there. The Passaúna basin underwent a dynamic due to the implementation of this reservoir, thus serving to test and validate the proposed methods.

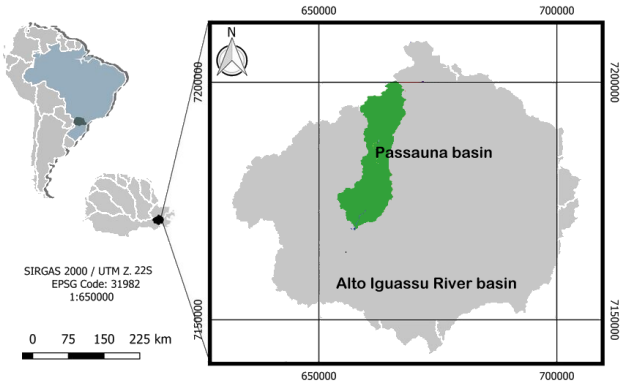

Figure 2 – Location of the Passaúna river basin within the Alto Iguassu basin. Adapted from Cipriano et al. (2019).

5. EXPERIMENTS

The Passaúna basin is contained in the 220/078 image within the Landsat reference system. The images from the years 1984, 1985, 1986, 1988, 1990, 2013, 2015-2020 were analysed. Images from different years were classified into the four NDVI ranges.

Figure 3 presents the histograms of NDVI images from the years 1988 and 2018 for comparative analysis. The 1988 image contains fewer negative values, as it was captured prior to the filling of the Passaúna Reservoir in September 1990. The figure also illustrates the proposed thresholds used for NDVI classification. The third range, which corresponds to healthy vegetation, consistently exhibits the highest peak across all images. This aligns with expectations, given that the watershed includes extensive rural and forested areas. However, it is important to note that the proportion of pixels within each NDVI range varies throughout the year, influenced by reflectance changes associated with the agricultural cycle.

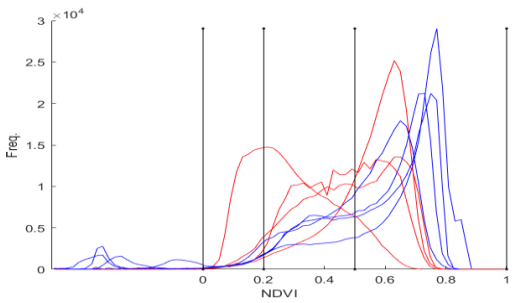

Figure 3 - NVDI histograms in the Passaúna basin (1988 red, 2018 blue).

Each image was summarized to a two-bit value, as shown in Table 1. Next, the binary codes of the four images from the same year were concatenated to produce an 8-bit representation, two for each month.

Table 1 - Variation of NDVI ranges throughout the year

Coverage	value	Binary code
High Vegetation (woods/ reforestation)	3	11
Low vegetation	2	10
Soil / Urban	1	01
Water	0	00

Binary encoding results in values between 0 and 255. However, not all values are present, as not all possible combinations are verified in practice. Therefore, the frequency of the coded values in the four images was analysed by inspecting the histograms of the four encoded images as shown in Figure 4. Values below 70 were disregarded, as they result from the presence of clouds or shadows on some dates.

Based on these histograms, the highest peaks were identified, as shown in Table 2, which characterize the most frequent temporal patterns. The values around 85 and 149 characterize regions predominantly occupied by class 1 (soil/urban|) in most of the year. Therefore, this ranges were grouped as being representative of a single class. Something similar is found for the ranges close to 154 and 170. Here, the most frequent value is 2 (low vegetation). A third class can be distinguished for values close to 218, characterized by the occurrence of “soil” on some dates, “low vegetation” on others, and “dense vegetation” on the last. This oscillation is typical of agriculture, so this range of values was interpreted as agricultural fields with typical variation of the phenological cycle and cultivation practices. Finally, values around 219-255 characterize areas of dense vegetation along the whole year.

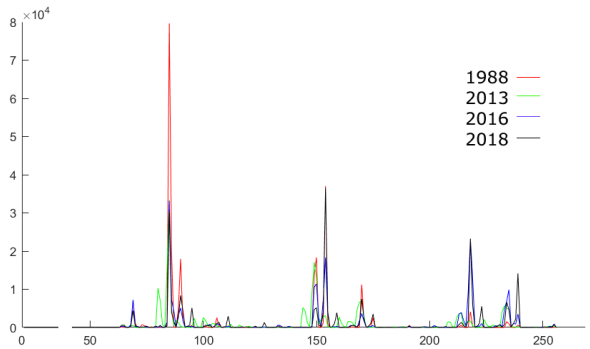

Figure 4- Histograms of the binary encoded images.

Table 2 - Most frequent binary codes

	code	Date 1	Date 2	Date 3	Date 4
85:	10 10 10 10	1	1	1	1
149:	10 10 10 01	1	1	1	2
154:	01 01 10 01	2	2	1	2
170:	01 01 01 01	2	2	2	2
218:	01 01 10 11	2	2	1	3
239:	11 11 01 11	3	3	2	3
255:	11 11 11 11	3	3	3	3

With these four classes, thematic maps showing the evolution of land cover in the basin were produced. Figure 4 compares the thematic maps of 1988 and 2013. There was an increase in dense vegetation in 2013, especially in the upper part of the basin and in the vicinity of the lake.

This contribution has been peer-reviewed. The double-blind peer-review was conducted on the basis of the full paper.
https://doi.org/10.5194/isprs-annals-X-3-W4-2025-63-2026 | © Author(s) 2026. CC BY 4.0 License.

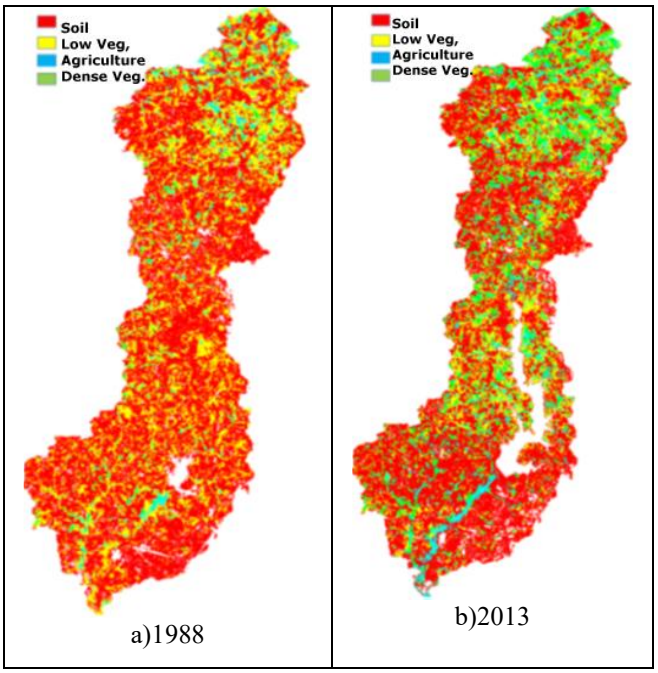

Figure 5 – Classification of coverage based on the binary code

The frequency histograms of these two images make this finding more evident, as shown in Figure 5. The increase in agricultural areas in 2013 and the reduction of areas characterized as soils is also evident. The increase in green areas in the central part of the basin can be explained because of the increase in humidity in the region near the new lake. The occupation of the basin by agriculture is also an expected phenomenon due to the expansion of economic activity in the basin, as displayed on Figure 6.

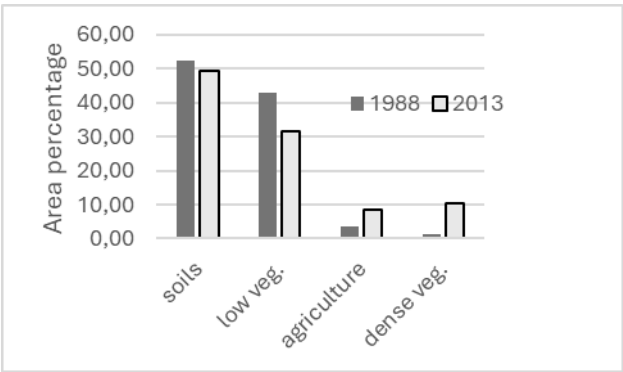

Figure 6 – Comparison of the frequency of classes in the basin in 1988 and 2013.

A similar analysis was performed for the years 2016 and 2018 to verify the stability of the values. The coded images are quite similar, as can be seen in figures 7 and 8. It should be noted that the 2016 image had small areas of shadow that cause grey round spots in the upper central part. The areas covered by each class were also analysed (Figure 9), concluding that there was a slight increase in agriculture to the detriment of areas of low vegetation. The areas occupied by dense vegetation remained practically stable.

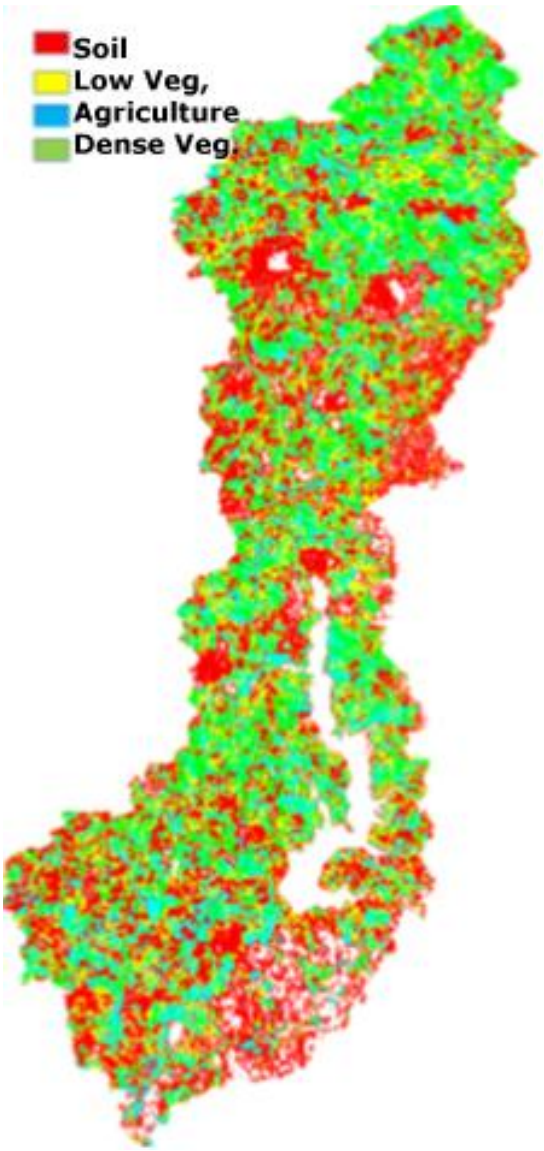

Figure 7 - Classification of coverage based on binary encoding in 2016.

In hydrological terms, the changes recorded between 2013 and 2018 show little variation in the infiltration potential, as the areas covered by dense vegetation apparently increased. However, this occurred in parallel with the increase in agriculture, which increases the potential for producing diffuse pollution. A comparison is displayed on Figure 9. In terms of infiltration, the increase of vegetation covered areas is positive. On the other hand, the increase of agricultural fields can be related to the increase of non-point pollution, increasing the rates of soil loss and pollutant production.

The changes recorded between 1988 and 2018 were very strong, but it was also noticed that the situation stabilized in the last years. The construction of the reservoir introduced changes, like new agriculture areas around the water body, but it was also noted that more dense vegetation areas appeared in the upper basin. These changes have strong influence on the infiltration rates and potential run-off. The analysis of the last decade shows little variation in the infiltration potential, as the areas covered by dense vegetation apparently increased. However,

this occurred in parallel with the increase in agriculture, which increases the potential for producing diffuse pollution.

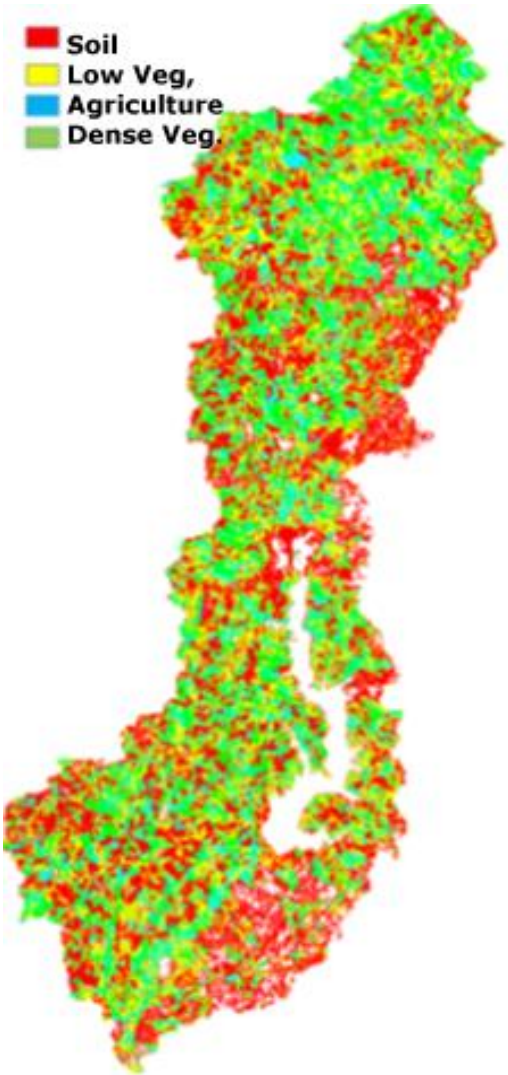

Figure 8 - Classification of coverage based on binary encoding in 2018.

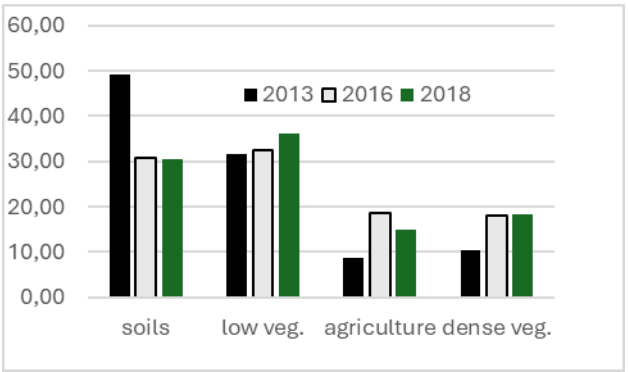

Figure 9 – Percentage of areas occupied by each class in the 2013, 2016 and 2018 images.

6. CONCLUSIONS

In this study, the use of binary coding was researched and evaluated to facilitate the analysis of the temporal variation of pixels throughout the year. The analysis of the Passaúna basin (PR/Brazil) was limited by the availability of images without cloud cover. Therefore, few images could be used. To map land cover classes with seasonal variation considering four dates, two bits were used per date. The product allowed separating more types of cover than considering only one index, because agriculture was differentiated from pastures/low vegetation due to its seasonal variation. This could also be valid in regions with deciduous forests, which is a type of forest that, at a certain time of the year, loses its leaves.

Binary encoding allowed mapping the evolution of cover resulting from the filling of the lake of the Passaúna reservoir and to locate where they occurred. The positive aspect of this approach is that it does not require the selection of training samples for the purpose of obtaining a rating. As the vegetation index is a normalized variable, the adoption of variation ranges allowed for the separation of some classes on each date and, when several dates were combined in the same year, the potential for discrimination increased, as it was possible to integrate the seasonal aspect.

The present study was restricted to four dates per year because of the image availability in the study region. When dealing with less cloud cover frequency, a longer binary chain can be constructed in a similar way, enabling a more detailed analysis of the yearly variation. It is therefore recommended to adapt apply the approach to longer yearly series, using other remote sensors, with higher temporal resolution, or combining several sensors, once the input is the segmented NDVI image.

REFERENCES

Bertucini Junior, J. J.; Silva Centeno, J. A. 2017. Detecção de alterações em alvos agrícolas e florestais empregando índices de vegetação em uma série multitemporal de imagens Landsat. *Revista Brasileira de Cartografia*, v. 69, n. 6.

Cai, S., Liu, D., 2015. Detecting Change Dates from Dense Satellite Time Series Using a Sub-Annual Change Detection *Algorithm Remote Sens*. 2015, 7, pp.8705-8727.

Chen J, Jönsson P, Tamura M, Gu ZH, Matsushita B, Eklundh L. 2004. A simple method for reconstructing a high-quality NDVI time-series data set based on the Savitzky-Golay filter. Remote Sens Environ. 2004;91(3–4):332–344.

Cipriano, F., Prado, L., Kozak, C., Fernandes, C., 2019. Consolidação de rotina analítica para quantificação de fósforo total em corpos hídricos: Impactos para a Gestão dos Recursos Hídricos. *REGA*, vol.16, nr. 13.

Elgammal, M., Rafat, A., Rasha, S., 2014. NDVI Threshold Classification for Detecting Vegetation Cover in Damietta Governorate. *J. Am. Sci.,* 10 (8) (2014), pp. 108-113.

Fu, Y., Zhu, Z., Liu, L., Zhan, W., He, T., Shen, H., Zhao, J., Liu, Y., Zhang, H., Liu, Z., Xue, Y., & Ao, Z. (2024). Remote Sensing Time Series Analysis: A Review of Data and Applications. Journal of Remote Sensing, 4, Article 0285. https://doi.org/10.34133/remotesensing.0285

Gross, D., 2005, Monitoring Agricultural Biomass Using NDVI Time Series. *Food and Agricultural Organisation of the United Nations* (FAO).

Hansen, M. C., Loveland, T. R., 2012. A Review of Large Area Monitoring of Land Cover Change Using Landsat Data. *Remote Sensing of Environment*, 122, 66-74.

Hashim, H., Latif, Z., Asnan, N., 2019. Urban vegetation classification with NDVI threshold value method with very high resolution (VHR) Pleiades imagery. *The International Archives of the Photogrammetry, Remote Sensing and Spatial Information Sciences*, Volume XLII-4/W16, 2019. 6th International Conference on Geomatics and Geospatial Technology (GGT 2019), 1–3 October 2019, Kuala Lumpur, Malaysia

Haywood, A., Verbesselt, J., Baker, P. J., 2016. Mapping disturbance dynamics in wet sclerophyll forests using time series LANDSAT. *The International Archives of the Photogrammetry, Remote Sensing and Spatial Information Sciences*, Volume XLI-B8, 2016. XXIII ISPRS Congress, 12–19 July 2016, Prague, Czech Republic.

Hu, Y., Huang, J., and Du, Y., 2015. Monitoring spatial and temporal dynamics of flood regimes and their relation to wetland landscape patterns in Dongting Lake from MODIS time-series imagery, *Remote Sensing*, 7(6), 7494-7520 (2015).

Jia, X., Richards, J. A., 1993. Binary coding of imaging spectrometer data for fast spectral matching and classification. *Remote Sensing of Environment* 43, pp. 47-53.

Jijón-Palma, M. E.; Amisse, C.; Silva Centeno, J. A. 2020. Multitemporal image encoding for monitoring spatiotemporal variations of water bodies using Landsat 8 Operational Land Imager (OLI) data. *Journal of Applied Remote Sensing*, v. 14, n. 3, p. 034523, 2020. DOI: 10.1117/1.JRS.14.034523.

Jianya. G., Haigang, S., Guorui, M., Qiming, Z., 2008. A review of multi-temporal remote sensing data change detection algorithms. *The International Archives of the Photogrammetry, Remote Sensing and Spatial Information Sciences*. Vol. XXXVII. Part B7. Beijing 2008.

Kennedy, R.E., Yang, Z., Cohen, W.B., 2010. Detecting trends in forest disturbance and recovery using yearly Landsat time series: 1. LandTrendr — Temporal segmentation algorithms. *Remote Sensing of Environment* 114 (2010) pp:2897–2910.

Leonardo, P., Franceisco, G., Jose, A., Sobrino, Juan, C., Jimenez, M., Haydee, K., 2006. Radiometric correction effects in Landsat multi-date/multisensor change detection studies, *International Journal of Remote Sensing*, 2, pp.685-704.

Li, S., Xu, L., Jing, Y., Yin, H., Li, X., & Guan, X. (2021). High-quality vegetation index product generation: A review of NDVI time series reconstruction techniques. *International Journal of Applied Earth Observation and Geoinformation*, 105, Article 102640

Ogilvie, A., Belaud, G., Massuel, S., 2018. Surface water monitoring in small water bodies: potential and limits of multi-sensor Landsat time series. *Hydrology and Earth System Sciences*, 22(8), 4349.

Rokni, K., Ahmad, A.,Selamat, A., 2014. Water feature extraction and change detection using multitemporal Landsat imagery. *Remote Sensing,* 6(5), 4173-4189.

Sheng, Y., Song, C. Wang, J., 2016. Representative lake water extent mapping at continental scales using multi-temporal Landsat-8 imagery. *Remote Sensing of Environment*, 185, 129-141.

Taravat, A., Rajaei, M., Emadodin, I., 2016. A spaceborne multisensory, multitemporal approach to monitor water level and storage variations of lakes. *Water*, 8(11), 478.

Townshend, J. R., Justice, C. O., 1986 Analysis of the dynamics of African vegetation using the normalized difference vegetation index, International Journal of Remote Sensing, 7(11), 1435-1445.

Tucker, C. J. , Sellers, P. J., 1986. Satellite remote sensing of primary production, *International Journal of Remote Sensing*, 7(11, 1395-1416.

USGS, 2023. Landsat Collection 1. Available at https://www.usgs.gov/landsat-missions/landsat-collection-1

Verbesselt, J., Hyndman , R,, Newnham,G., Culvenor, D., 2010. Detecting trend and seasonal changes in satellite image time series. *Remote Sensing of Environment* 114 (2010 PP.106–115.

Xie, H., Heipke, C., Lohmann, P., Soergel, U., Tong, X., 2011. A new binary encoding algorithm for the simultaneous region-based classification of hyperspectral data and digital surfase models. *Photogrammetrie Fernekundung Geoinformation*, v. 1.

Yao, F., Wang, C., Dong, D., 2015. High-resolution mapping of urban surface water using ZY-3 multi-spectral imagery,"*Remote Sensing*, 7(9, 12336-12355.

Yao, F., Wang, J., Wang, C., 2019. Constructing long-term high-frequency time series of global lake and reservoir areas using Landsat imagery. *Remote Sensing of Environment*, 232, 111210.